Adaptive Impulsive Noise Removal in Color Images

Bogdan Smolka
Silesian University of Technology, Department of Automatic Control,
Akademicka 16, 44-100 Gliwice, Poland
E-mail: smolka@ieee.org Tel: +48-32-2371912

***Abstract*—In this paper a novel adaptive filtering scheme for impulsive noise removal in color images is presented. The noise detection algorithm is based on the concept of aggregated distances assigned to the pixels belonging to the filtering window. The value of the difference between the accumulated distance assigned to the central sample and to the pixel with the lowest rank serves as an indicator of the presence of impulses injected into the image by the noise process and adaptively influences the filter output which is a weighted mean of the central pixel of the filtering window and the vector median of its samples.**

The obtained results show that the proposed filter outperforms existing impulse noise removal techniques for low noise contamination and can be used in various applications in which the detail preserving reduction of impulses plays an important role.

I. Introduction

The amount of research published in the last years indicates a growing interest in the area of color image processing and analysis. Furthermore, the surge of emerging applications such as web-based processing of color images and videos, image retrieval systems indexing large multimedia databases, enhancement and understanding of medical and biological images, digital archiving, cultural heritage preservation projects and the proliferation of smart devices such as video-enabled wireless phones, wearable computers and personal digital assistant tools, suggests that the demand for new, more powerful and cost effective multichannel filtering solutions will continue.

Computer vision systems very often use color information to sense the environment and therefore the correct processing of color information is of great importance in various tasks of pattern recognition and image understanding. Unfortunately, noise and other impairments associated with the acquisition and transmission can significantly degrade the value of the color information carried by digital images. This usually declines their perceptual fidelity and also decreases the performance of the task for which the image was created.

It comes therefore as no surprise that the most common signal processing task is noise filtering. The reduction of noise is an essential part of any image processing based system, whether the final information is used for human perception or for an automatic inspection and analysis [1].

The correction of the signal distortions is a process, in which disturbances introduced by the sensors are rectified, with the goal being to obtain the image or generally the signal, which corresponds as closely as possible to the output of an ideal imaging system. Thus, correcting signal artifacts, in practice means adjusting the characteristics of the imaging system to meet specific demands of the human observer or the computer vision system.

During image *formation*, *acquisition*, *storage* and *transmission* many types of distortions limit the quality of digital images. Transmission errors, periodic or random motion of the camera system during exposure, electronic instability of the image signal, electromagnetic interferences, sensor malfunctions, optic imperfections or aging of the storage material, all disturb the image quality. In many practical situations, images are corrupted by the so called *impulsive noise* caused mainly either by faulty image sensors or due to transmission errors resulting from man-made phenomena such as ignition transients in the vicinity of the receivers or even natural phenomena such as lightning in the atmosphere.

In this paper the problem of impulsive noise removal in color images is addressed and an efficient adaptive technique capable of removing the impulsive noise and preserving important image features is proposed.

The paper is organized as follows. In the next section a short overview of the basic multichannel filtering schemes is provided. Then the new filtering approach is introduced and its similarity to existing filtering schemes is discussed. Section III presents the construction of the new adaptive filtering scheme and section IV covers the experimental results performed on the test images contaminated with impulsive noise. The paper ends with a short conclusion.

II. Vector Median Based Filters

A multichannel image is a mapping $\mathbb{Z}^2 \rightarrow \mathbb{Z}^m$ representing a two-dimensional matrix of of size $N_1 \times N_2$ consisting of m-component samples (pixels), $\boldsymbol{x}_i = (x_{i1}, x_{i2}, \ldots, x_{im}) \in \mathbb{Z}^l$, where m denotes the number of channels, (in the case of standard color images, parameter m equals 3). Components x_{ik}, for $k = 1, \ldots, m$ and $i = 1, 2, \ldots, N$, $N = N_1 \cdot N_2$, represent the color channel values quantified into the integer domain..

The majority of the nonlinear, multichannel filters intend for the suppression of impulse noise in color images are based on the ordering of vectors in a sliding filter window. The output of these filters is defined as the lowest ranked vector according to a specific vector ordering technique [2], [3].

Let the color images be represented in the commonly used RGB space and let $\{\boldsymbol{x}_1, \boldsymbol{x}_2, \ldots, \boldsymbol{x}_n\}$ be 3-dimensional samples from the sliding filter window W, with $\boldsymbol{x}_1$ being the central element in W. The goal of the vector ordering is to

arrange the set of n vectors $\{\boldsymbol{x}_1, \boldsymbol{x}_2, \ldots, \boldsymbol{x}_n\}$ belonging to W using some sorting criterion.

The most widely used ordering scheme is based on the aggregated distances assigned to the samples belonging to the filtering window defined as

$$r_i = \sum_{j=1}^{n} \rho(\boldsymbol{x}_i, \boldsymbol{x}_j)\,, \tag{1}$$

where $\rho(\boldsymbol{x}_i, \boldsymbol{x}_j)$ is the distance between the vectors $\boldsymbol{x}_i$ and $\boldsymbol{x}_j$. The increasing ordering of the scalar quantities $\{r_1, r_2, \ldots, r_n\}$ generates the ordered set of vectors $\{\boldsymbol{x}_{(1)}, \boldsymbol{x}_{(2)}, \ldots, \boldsymbol{x}_{(n)}\}$.

One of the most important noise reduction techniques is the *Vector Median Filter* (VMF), whose output is the vector $\boldsymbol{x}_{(1)}$ from W for which the sum of distances to all other vectors belonging to W is minimized and it satisfies, (see Fig. 1) [2]

$$\sum_{j} \rho\left(\boldsymbol{x}_{(1)}, \boldsymbol{x}_j\right) \leq \sum_{j} \rho\left(\boldsymbol{x}_i, \boldsymbol{x}_j\right), \quad \boldsymbol{x}_i, \boldsymbol{x}_j \in W\,. \tag{2}$$

The Vector Median Filter (VMF) is the most popular vectorial operator intended for smoothing out spikes injected into the color image by the impulse noise process. This filter is very efficient at reducing the impulses, preserves sharp edges and linear trends, however it does not preserve fine image structures, which are treated as noise and therefore generally the VMF tends to produce blurry images.

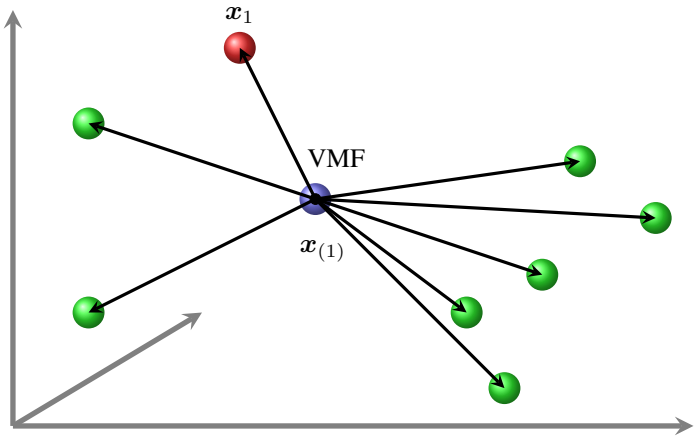

Fig. 1: The VMF output is the centrally located vector $\boldsymbol{x}_{(1)}$.

The VMF concept has been generalized and the so-called *Weighted Vector Median Filter* (WVMF) has been proposed [4], [5]. Using the *weighted vector median* approach, the filter output is the vector $\boldsymbol{x}_{(1)}$ belonging to W, for which the following condition holds

$$\sum_{j=1}^{n} \psi_j\, \rho\left(\boldsymbol{x}_{(1)}, \boldsymbol{x}_j\right) \leq \sum_{j=1}^{n} \psi_j\, \rho\left(\boldsymbol{x}_i, \boldsymbol{x}_j\right), \quad \boldsymbol{x}_i, \boldsymbol{x}_j \in W\,. \tag{3}$$

where ψ_j, $j = 1, \ldots, n$ are weights assigned to the pixels $\boldsymbol{x}_j$ from W. If $\psi_1 > 1$ and $\psi_k = 1$ for $k = 2, \ldots, n$, ($\boldsymbol{\psi} = \{\psi_1, 1, 1 \ldots, 1\}$), then the *Central Weighted VMF* (CWVMF) which privileges the pixel $\boldsymbol{x}_1$ is obtained [5]–[7]. The CWVMF has the ability of noise removal, while preserving better fine image details, (lines, edges, corners, texture) and significantly outperforming the standard VMF.

The drawback of the filtering methods based on the ordering of samples according to the values of the aggregated distances is that the derived filters operate uniformly over the image and unnecessary replace pixels which were not corrupted by the noise process.

To alleviate this drawback many switching mechanisms were introduced into the structure of the impulsive noise reduction filters [8], [9]. The goal of a switching filtering scheme is to efficiently detect the noisy pixels and to replace them by a noise removal filter output, while preserving the uncorrupted samples.

An extension of the VMF, in which an adaptive switching filtering design was utilized, was proposed in [10]. This switching design, based on the order statistics and relying on a thresholding parameter, suppresses efficiently impulsive noise present in color images, while preserving the image details.

In [11]–[14] adaptive switching techniques were introduced. The major advantage of these methods is that they filter out the noise component while adapting itself to the local image structures and in this way they are able to eliminate strong impulsive noise while preserving edges and retaining fine image details. As these algorithms can be treated as fuzzy modifications of the commonly used vector median, they are fast and easy to implement.

In order to avoid excessive blurring of images during the filtering process, the *Signal Dependent Rank-Ordered Mean* (SD-ROM) filter was proposed [15]. In the SD-ROM approach, the filtering operation is conditioned on the differences between the input pixel and its rank-ordered neighbors from W. The filter yields satisfactory results, however its thresholding parameters are dependent on the noise intensity and thus a proper settings of the thresholds is required.

In [16] a switching scheme based on the local energy derived from on the Teager-like operator was described [17]. The pixels of the color image whose energy exceed a local threshold are being detected as outliers and replaced in this scheme by the median of the RGB color image channels.

Another scheme proposed in [18] divides the pixels of the filtering window into two groups. The first one consists of the pixels similar to the central pixel $\boldsymbol{x}_1$ and the other one is composed of those pixels, which deviate greatly in terms of the Euclidean distance from $\boldsymbol{x}_1$. The division into the two classes of pixels is performed utilizing the Fisher linear discriminant, which enables the labeling of the central pixel as noisy or undisturbed by noise process.

Another approach described in [19], [20] divides the set of pixels in the filtering window using the extension of the concept of the σ-filtering. The measure of the dispersion of the input pixels is calculated as the mean sum of distances between the output of the VMF and all other pixels in W. In this way a fast and robust modification of the VMF can be realized.

III. Proposed Filtering Design

The well known local statistic filters constitute a class of linear minimum mean squared error estimators and they make use of the local mean and variance of the input set $W = \{x_1, x_2, \ldots, x_n\}$ defining the filter output for the gray-scale images as [21], [22]

$$y_i = \hat{x}_i + \alpha\,(x_i - \hat{x}_i) = \alpha x_i + (1-\alpha)\hat{x}_i\,, \tag{4}$$

where $\hat{x}_i$ is the arithmetic mean of the image pixels belonging to the filtering window W centered at a pixel position i and α is a filter parameter usually estimated through [6]

$$\alpha = \frac{\sigma_x^2}{\sigma_n^2 + \sigma_x^2}\,,\ \hat{x}_i = \frac{1}{n}\sum_{j=1}^{n} x_j\,,\ \nu^2 = \frac{1}{n}\sum_{j=1}^{n}(x_j - \hat{x}_i)^2\,,$$

$$\sigma_x^2 = \max\left\{0, \nu^2 - \sigma_n^2\right\},\ \alpha = \max\left\{0, 1 - \sigma_n^2/\nu^2\right\}\,, \tag{5}$$

where ν^2 is the local variance calculated from the samples in W and σ_n^2 is the estimate of the variance of the noise process. If $\nu \gg \sigma_n$, then $\alpha \approx 1$ and practically no changes are introduced. When $v < \sigma_n$, then $\alpha = 0$ and the central pixel is replaced with the local mean. In this way, the filter smooths with the local mean, when the noise is not very intensive and leaves the pixel value unchanged, when a strong signal activity is detected. The major drawback of this filter is that it fails to remove impulses and leaves noise in the vicinity of edges.

Equation (4) can be rewritten using the notation $x_i = x_1$, (x_1 is the central sample in W), [6] as

$$\begin{aligned} y_1 &= \alpha x_i + (1-\alpha)\hat{x}_i = \alpha x_1 + (1-\alpha)\hat{x}_1 = \\ &= (1-\alpha)\left(\psi_1 x_1 + x_2 + \ldots + x_n\right)/n, \end{aligned} \tag{6}$$

with $\psi_1 = (1 - \alpha + n\alpha)/(1-\alpha)$ and the local statistic filter defined by (4) is reduced to the *central weighted average*, with a weighting coefficient ψ_1. In this way the set of weights $\{\psi_1, 1, 1, \ldots, 1\}$ is assigned to the set of pixels in the filtering window $\{x_1, x_2, \ldots, x_n\}$

$$y_1 = \frac{1}{n + \psi_1 - 1}\sum_{k=1}^{n}\psi_k x_k\,, \tag{7}$$

If the weighting is applied to the ordered sequence of gray-scale samples belonging to W: $\{x_{(1)}, \ldots, x_{(\mu)}, \ldots, x_{(n)}\}$, where $x_{(1)}$ and $x_{(n)}$ are the minimal and maximal pixel values and $x_{(\mu)}$, ($\mu = (n+1)/2$) denotes the median of the input set, then

$$y_1 = \frac{1}{\sum_{k=1}^{n}\psi_k}\sum_{k=1}^{n}\psi_k x_{(k)}\,. \tag{8}$$

Taking the weighting set $\{1, 1, \ldots, \psi_\mu, \ldots, 1\}$, special emphasis is given to the median of the input set $x_{(\mu)}$. Hence

$$\begin{aligned} y_1 &= \left(\frac{n}{n + \psi_\mu - 1}\right)\hat{x}_1 + \left(\frac{\psi_\mu - 1}{n + \psi_\mu - 1}\right)x_{(\mu)} = \\ &= (1-\alpha)\hat{x}_1 + \alpha x_{(\mu)}\,, \end{aligned} \tag{9}$$

which is a compromise between the median $x_{(\mu)}$ and the average $\hat{x}_1$ controlled again by the parameter α.

Let us now apply a weighting structure defined by the weights $\{1, 0, \ldots, \psi_\mu, \ldots, 0\}$. Such a setting of the weights leads to the output defined by

$$y_1 = \frac{1}{1+\psi_\mu}\left(x_1 + \psi_\mu x_{(\mu)}\right) = \alpha x_1 + (1-\alpha)x_{(\mu)}\,. \tag{10}$$

If we work on the set of ordered vectors $\{\boldsymbol{x}_{(1)}, \boldsymbol{x}_{(2)}, \ldots, \boldsymbol{x}_{(n)}\}$ then (10) can be rewritten as

$$y_1 = \frac{1}{1+\psi_1}\left(\boldsymbol{x}_1 + \psi_1 \boldsymbol{x}_{(1)}\right) = \alpha \boldsymbol{x}_1 + (1-\alpha)\boldsymbol{x}_{(1)}\,, \tag{11}$$

where the weighting set is defined as: $\{\psi_1, 0, \ldots, 0, 1, 0, \ldots, 0\}$ in which the weight ψ_1 is assigned to the *vector median* $\boldsymbol{x}_{(1)}$ of the input set from W and 1 is assigned to the central pixel $\boldsymbol{x}_1$.

Clearly, the filtering structure defined by (11) is similar to approaches defined by (4), (6) and (9). However, as our aim is to construct a filter capable of removing impulsive noise, instead of the mean value, the VMF output is utilized and the noise intensity estimation mechanism is accomplished through the coefficient α, which should be adjusted to the noise contamination level.

In this way, the proposed technique is a compromise between the VMF and the identity operation. When an impulse is present, then the value of α should be 0, otherwise it should be 1. It is interesting to observe that the filter output $\boldsymbol{y}_i$ lies on the line joining the vectors $\boldsymbol{x}_1$ and $\boldsymbol{x}_{(1)}$ and depending on the value of α, it slides from the identity operation ($\boldsymbol{x}_1$) to the vector median ($\boldsymbol{x}_{(1)}$) [23], [24].

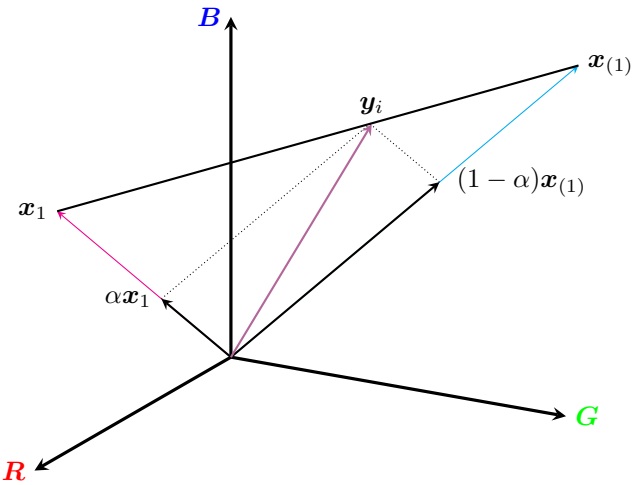

Fig. 2: Construction of the filter output as a weighted mean of the central pixel $\boldsymbol{x}_1$ and the vector median $\boldsymbol{x}_{(1)}$.

The filtering efficiency of the proposed scheme depends strongly on the accuracy of the impulse detection. The straightforward choice would be to detect the impulses by measuring the difference between the central pixel of the filtering window and the vector median of its samples. However, such an approach is not suitable for noise detection, as the image texture and edges can be easily treated as noise, which leads

to extensive image smoothing, caused by unnecessary pixel replacement by the vector median.

The proposed switching filter is based on the difference between the aggregated distance r_1 assigned to the central pixel of the filtering window and the value of $r_{(1)}$ corresponding to the vector median output. Introducing the notation: $r_1 = r_c$ and $r_{(1)} = r_m$, the measure of pixel distortion r_d is then expressed as: $r_d = r_c - r_m$.

Figure 3 shows examples of the detected noise using parts of the test images LENA and GOLDHILL. The visual comparison of the noise map composed of the values of r_d and the differences between the noisy and original test images, confirms the good noise detection ability of the proposed approach. The map of the detected noise corresponds very well with the real corruption derived from the noisy and clean images.

To discriminate between pixels corrupted by impulse noise and the undisturbed samples, a global thresholding scheme could be applied. However, the thresholding of the noise map would lead to many errors which would result in retaining the impulses and unnecessary undisturbed pixel replacement. To alleviate the problems connected with hard thresholding, a soft scheme has been applied. Utilizing the filtering framework defined in Eq. (11), we can use the noise map as a distortion measure and make the α coefficient to be dependent on the values of the noise intensity r_d. In this way, every pixel will be replaced by the weighted mean of the central pixel of W and its vector median.

Of course, the efficiency of such a scheme depends heavily on the proper choice of the α coefficient. Experimental results indicates that satisfactory results can be achieved using various kernel functions known from the nonparametric estimation theory. Therefere, for the presentation of the filter efficiency the following form of the α coefficient has been chosen

$$\alpha = \exp\left\{-\left(\frac{r_d}{h}\right)^2\right\}, \tag{12}$$

where h is a normalization parameter.

IV. Experiments

In order to evaluate the effectiveness of the novel switching filter a set of test images (Fig. 4) was contaminated with three kinds of impulsive noise. In the first two noise models, the noisy pixels $\boldsymbol{x}_i = \{x_{i1}, x_{i2}, x_{i3}\}$ are defined as

$$x_{iq} = \begin{cases} \rho_{iq}\,, & \text{with probability } \pi\,, \\ o_{iq}\,, & \text{with probability } 1-\pi\,, \end{cases} \tag{13}$$

where o_{iq} denotes the q-th component of the original pixel at position i and the contamination component ρ_{iq} is a random variable.

If the variable ρ can take any discrete value in the range $[0, 255]$ the *uniform* or *random-valued* impulsive noise model is obtained, which will be denoted in this paper as α, (this kind of noise was used to contaminate the test images presented in Fig. 3). If ρ takes only the value 0 or 255, the *salt & pepper* or *fixed-valued* impulse noise is modeled and it will be denoted as β. The third kind of noise denoted as γ is defined as [1], [8], [9]

$$\boldsymbol{x}_i = \begin{cases} \boldsymbol{o}_i, & \text{with probability } 1-p, \\ \{\rho_{i1}, o_{i_2}, o_{i_3}\}, & \text{with probability } p_1\,p, \\ \{o_{i_1}, \rho_{i2}, o_{i_3}\}, & \text{with probability } p_2\,p, \\ \{o_{i_1}, o_{i_2}, \rho_{i3}\}, & \text{with probability } p_3\,p, \\ \{\rho_{i4}, \rho_{i4}, \rho_{i4}\}, & \text{with probability } p_4\,p, \end{cases} \tag{14}$$

where p is the noise intensity and p_1, p_2, p_3 are corruption probabilities of each color channel, so that $\sum_1^4 p_\kappa = 1$. The variables $\rho_{i\kappa}$, $\kappa = 1, \ldots, 4$ take on the value 0 or 255 with equal probability. In this work, the noise model γ will generally denote the case with $p_\kappa = 0.25$ for $\kappa = 1, \ldots, 4$. The three noise types are depicted in Fig. 5.

Fig. 4: Test images used for the simulations.

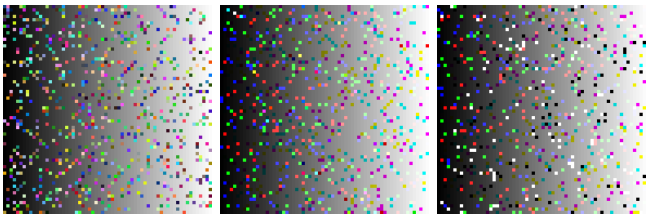

(a) NM α (b) NM β (c) NM γ

Fig. 5: visualization of the applied noise models.

For the measurement of the restoration quality, the commonly used *Mean Squared Error* (MSE) expressed through the *Peak Signal to Noise Ratio* (PSNR) was used, as the MSE (denoted here as ς) is a good measure of the efficiency of impulsive noise suppression. The PSNR is defined as

$$PSNR = 20\log_{10}\left(\frac{255}{\sqrt{\varsigma}}\right), \quad \varsigma = \frac{\sum_{i=1}^{N} \|\boldsymbol{x}_i - \boldsymbol{o}_i\|_2^2}{N}, \tag{15}$$

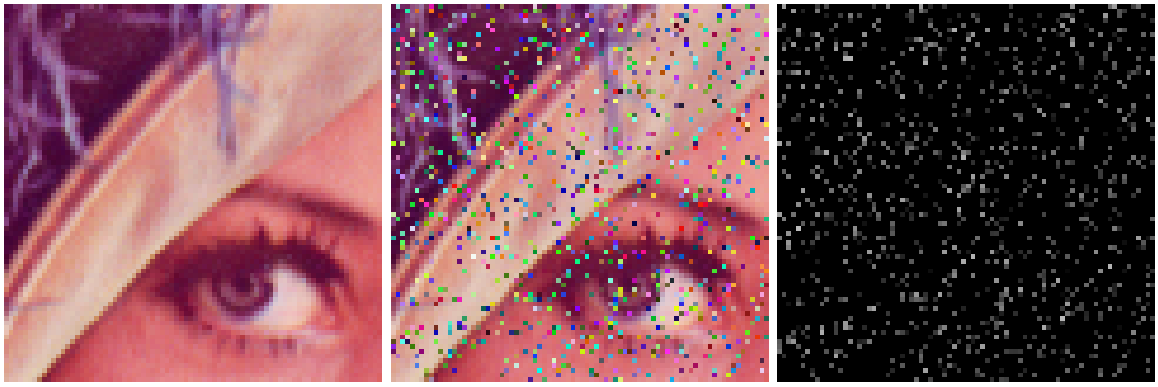

(a) original image (b) noisy image (c) real contamination

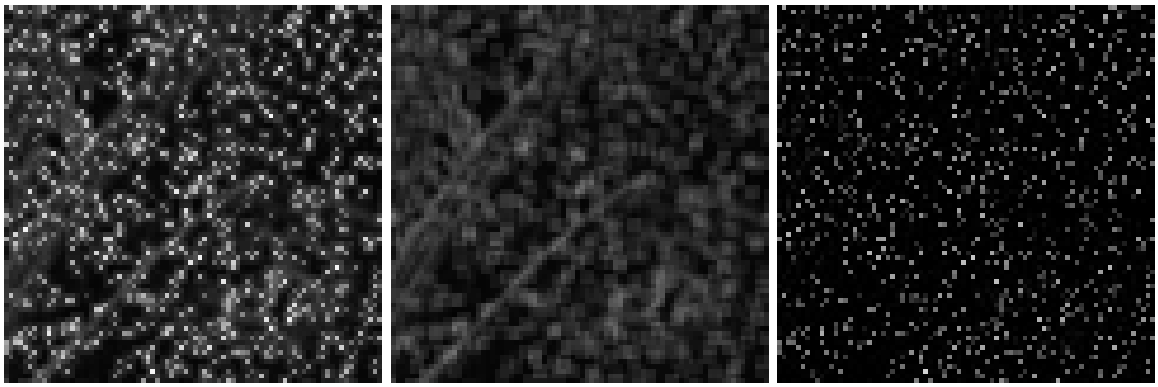

(d) map of r_c (e) map of r_m (f) detected noise: $r_c - r_m$

(g) original image (h) noisy image (i) real contamination

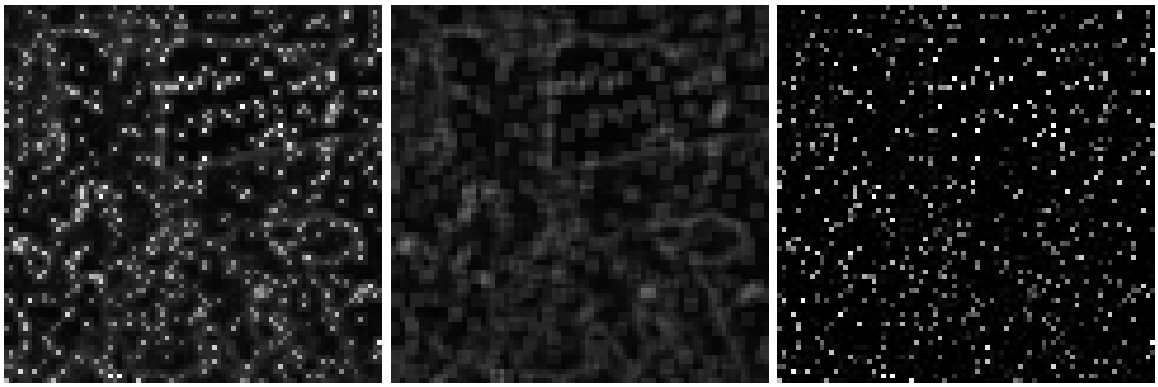

(j) map of r_c (k) map of r_m (l) detected noise: $r_c - r_m$

Fig. 3: Illustration of the noise detection scheme: parts of test images LENA and GOLDHILL (a), (g) and their noisy versions (b), (h) together with the difference of the images showing the injected impulse noise (c), (i). Below the maps of r_c, r_m and their difference $r_d = r_c - r_m$ is presented. Note the similarity between (c) and (f) and also between images (i) and (l).

where N is the total number of image pixels, and x_{iq}, o_{iq} denote the q-th component of the noisy image pixel channel and its original, undisturbed value at a pixel position i, respectively.

For the evaluation of the detail preservation capabilities of the proposed filtering design the *Mean Absolute Error* (MAE) has been used

$$MAE = \frac{1}{N}\sum_{i=1}^{N} \|\boldsymbol{x}_i - \boldsymbol{o}_i\|_1 , \tag{16}$$

where $\|\cdot\|_l$ denotes the kind of the used Minkowski norm.

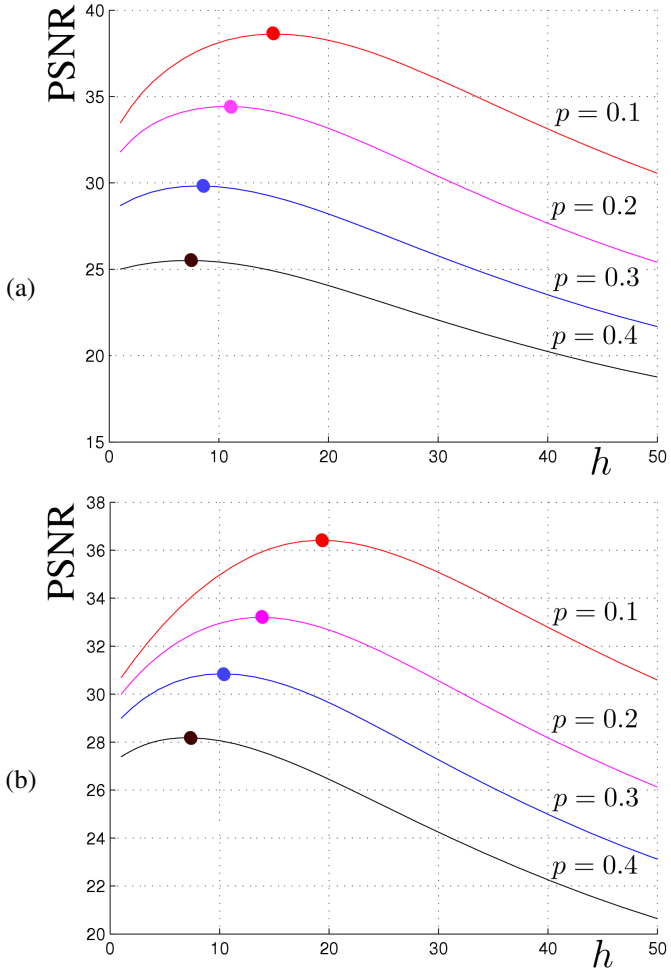

Fig. 6: Dependence of the PSNR on the h parameter for the LENA (a) and GOLDHILL (b) test images. The dots show the maxima of the plots and indicate the optimal h values for which the plots attain their maxima.

Figure 6 shows the dependence of the PSNR on the h smoothing parameter for two test images contaminated by the noise model α. As can be observed, the optimal value of the smoothing parameter h in Eq. 12, for which the PSNR measure attains the maximal value depends significantly on the contamination level p defined as the percentage of corrupted pixels.

Figure 7 shows the histograms of the contaminated GOLDHILL image composed of the values of r_c, r_m and r_d for increasing noise intensity. As can be seen by a comparison of the histograms, with increasing noise level p, the histograms are shifted towards higher values, which is confirmed by plots depicted in Fig. 8, which show the mean values of r_c, r_m and r_d denoted as $\hat{r}_c$, $\hat{r}_m$ and $\hat{r}_d$ evaluated for two test images. Additionally, the increase of the mean values of the r_d is linearly dependent on the noise level p, which enables to estimate the noise level knowing the mean value of $\hat{r}_d$ derived from its histogram. Figure 9 depicts that the linear dependence of r_d is similar for the commonly used test images (Fig. 4).

Figure 10 shows the dependence of the optimal value of the inverse of the optimal smoothing parameter, which will be denotes $h^* = 1/h$ on the noise intensity p. This dependence is also of linear character, which enables to combine the values of $\hat{r}_d$ and h^* as they are both linearly dependent on the noise intensity. This observation is confirmed by Fig. 11, which shows a linear dependence between the values of $\hat{r}_d$ and h^* which allows for adaptive tuning of the α parameter according to the noise intensity level. This behavior is quite important as it can be used for other denoising techniques requiring the estimation of the noise intensity in order to achieve optimal filtering efficiency.

The experimentally found formula allowing to estimate the optimal normalization parameter h is then

$$h^* = 0.00398 \cdot \hat{r}_d + 0.0177, \quad h^* = 1/h, \tag{17}$$

The effectiveness of the proposed filtering design was compared with a set of the most efficient noise removal switching filters evaluated in the extensive survey [25]:

- *Adaptive Center-Weighted Directional Distance Filter*, (ACWDDF), [26],
- *Peer Group Filter*, (PGF), [27],
- *Sigma Directional Distance Filter based on Rank*, (SDDFr), [28],
- *Adaptive Center-Weighted Vector Median Filter*, (ACWVMF) [26],
- *Adaptive Center-Weighted Vector Directional Filter*, (ACWVDF), [26],
- *Modified Center-Weighted Vector Median Filter*, (MCWVMF), [29],
- *Sigma Directional Distance Filter based on Mean*, (SDDFm), [28],
- *Sigma Vector Median Filter based on Rank*, (SVMFr), [28],
- *Fast Fuzzy Noise Reduction Filter*, (FFNRF), [30].

Analyzing the plot presented in Fig. 14 which shows the filtering results obtained for the test color image RAFTING contaminated with uniform noise of intensity 0.05, 0.1 and 0.15 it is clear that the proposed filtering approach significantly outperforms in terms of the PSNR measure the most efficient filtering designs known in the literature [25]. The MAE measure is similar to the analyzed filters, which is due to the smoothing introduced by the VMF in the applied weighting

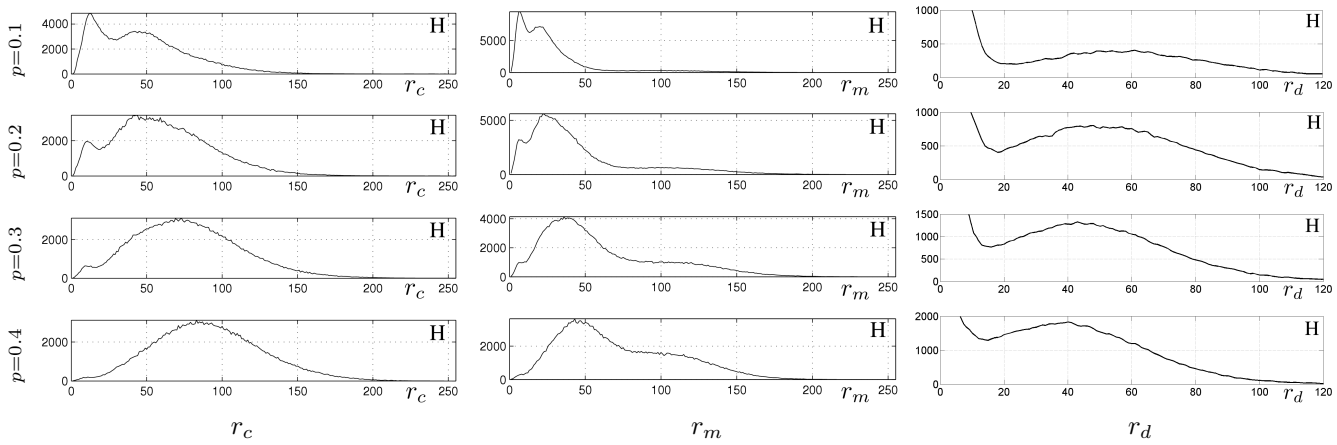

Fig. 7: Histograms of the maps of r_c, r_m and r_d for the GOLDHILL image contaminated by the uniform impulse noise.

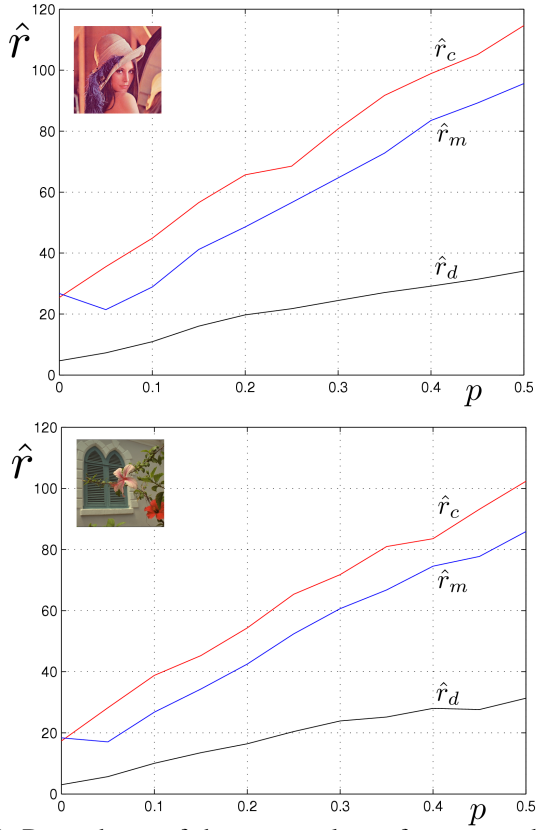

Fig. 8: Dependence of the mean values of r_m, r_c and r_d on the noise intensity p for the LENA and FLOWER test images.

TABLE I: Comparison of the filtering efficiency of the proposed filter as compared with the best filters evaluated in [25] for the *RAFTING*, *LOCOMOTIVE* and *MOTORBIKES* test images contaminated by the uniform noise

image		*RAFTING*		*LOCOMOTIVE*		*MOTORBIKES*	
FILTER	p	MAE	PSNR	MAE	PSNR	MAE	PSNR
PROPOSED	0.05	1.02	35.07	3.14	26.87	1.23	33.47
	0.10	1.43	33.44	4.05	25.64	1.79	31.49
	0.15	1.82	32.26	4.81	24.81	2.33	30.22
ACWDDF	0.05	0.97	34.51	2.43	27.17	1.23	32.86
	0.10	1.30	33.31	2.94	26.55	1.62	31.64
	0.15	1.62	32.33	3.45	25.90	2.04	30.51
PGF	0.05	0.75	33.81	3.49	25.16	1.09	31.69
	0.10	1.13	32.42	4.16	24.58	1.60	30.29
	0.15	1.54	30.95	4.84	23.97	2.14	29.07
$SDDF_r$	0.05	1.13	33.69	2.74	26.64	1.07	33.22
	0.10	1.24	33.30	2.82	26.63	1.33	32.17
	0.15	1.45	32.36	3.05	26.23	1.67	30.90
ACWVMF	0.05	0.73	33.72	3.27	25.04	1.08	31.28
	0.10	1.06	32.68	3.71	24.71	1.48	30.29
	0.15	1.41	31.57	4.14	24.33	1.92	29.33
ACWVDF	0.05	1.25	32.58	2.73	26.47	1.64	30.63
	0.10	1.63	31.59	3.35	25.62	2.14	29.28
	0.15	2.02	30.49	3.99	24.80	2.66	28.19
MCWVMF	0.05	0.69	33.93	1.45	28.09	0.65	32.38
	0.10	1.08	30.95	2.01	25.99	1.19	29.08
	0.15	1.64	28.02	2.71	24.13	1.89	26.43
$SDDF_m$	0.05	1.67	32.44	3.64	25.80	1.73	31.34
	0.10	1.77	32.02	3.67	25.82	1.99	30.51
	0.15	1.99	30.93	3.92	25.37	2.33	29.35
$SVMF_r$	0.05	1.40	32.58	3.39	25.53	1.39	31.12
	0.10	1.48	32.14	3.54	25.21	1.61	30.28
	0.15	1.67	31.17	3.79	24.70	1.95	29.08
FFNRF	0.05	0.89	32.28	4.18	23.33	1.28	29.95
	0.10	1.23	31.43	4.61	23.09	1.68	29.15
	0.15	1.58	30.48	4.99	22.84	2.11	28.33

scheme of the proposed filter. The excellent behavior of the new filter is also confirmed in Tab. I which summarizes the results obtained for the RAFTING, LOCOMOTIVE and MOTORBIKES test images. The subjective analysis of the filtering results offered by the new filter and the methods used for comparisons is provided in Fig. 13, which shows the restored *RAFTING* image. As can be observed the new technique removes the impulses injected by the noise process and preserves the fine image details.

V. Conclusions

In the paper an adaptive filtering design for impulsive noise removal is proposed. The proposed noise detector together with the adaptive scheme of choosing the optimal value of the weighting parameter used in the construction of the filter exhibits very good denoising properties outperforming the known filtering solutions. The simplicity of the new algorithm and its computational speed makes the noise removal method

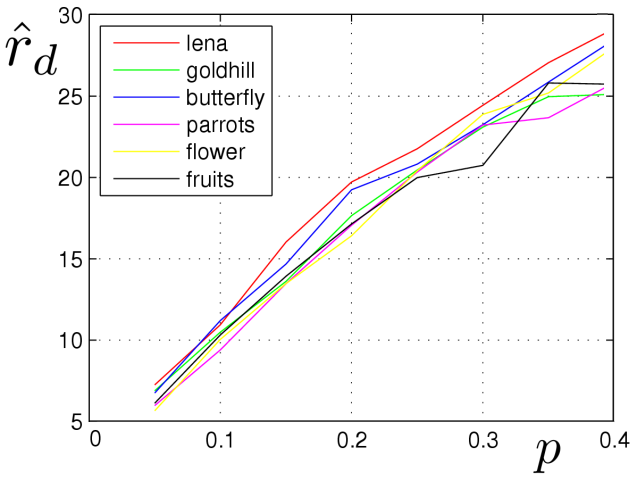

Fig. 9: Dependence of $\hat{r}_d$ on the noise intensity p.

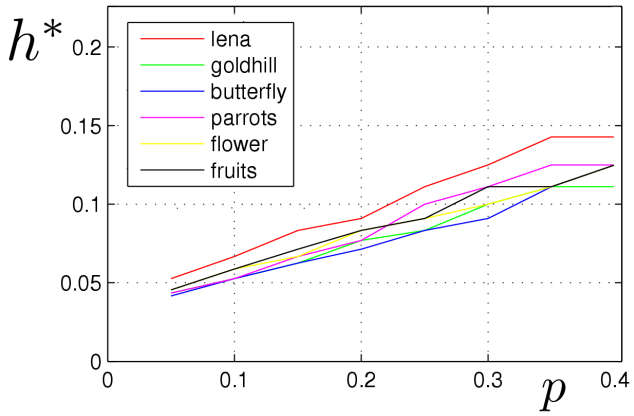

Fig. 10: Dependence of the optimal parameter h^* on p.

very useful in the preprocessing of color images corrupted by impulse noise.

REFERENCES

[1] K.N. Plataniotis and A.N. Venetsanopoulos, *Color Image Processing and Applications*, Springer Verlag, August 2000.

[2] J. Astola, P. Haavisto and Y. Neuvo, "Vector median filters," *Proc. of the IEEE*, vol. 78, no. 4, 1990, pp. 678-689.

[3] R. Lukac, B. Smolka, K. Martin, K.N. Plataniotis and A.N. Venetsanopoulos, "Vector filtering for color imaging," *IEEE Signal Processing Magazine*, Special Issue on Color Image Processing, vol. 22, no. 1, pp. 74-86, 2005.

[4] T. Viero, K. Öistämö and Y. Neuvo, "Three-dimensional median-related filters for color image sequence filtering," *IEEE Trans. on Circiuts and Systems for Video Technology*, vol. 4., no. 2, 1994, pp. 129-142.

[5] S.J. Ko and Y.H. Lee, "Center weighted median filters and their application to image enhancement," *IEEE Trans. on Circuits and Systems*, vol. 38, no. 9, 1991, pp. 984-993.

[6] T. Sun, M. Gabbouj and Y. Neuovo, "Center weighted median filters. Some properties and applications in image processing," *Signal Processing*, vol. 35, 1994, pp. 213-229.

[7] T. Chen and and H.R. Wu, "Adaptive impulse detection using center-weighted median filters," *IEEE Signal Processing Letters*, vol. 8, no. 1, 2001, pp. 1-3.

[8] B. Smolka, K.N. Plataniotis and A.N. Venetsanopoulos, "Nonlinear techniques for color image processing,", in "Nonlinear Signal and Image Processing: Theory, Methods, and Applications", pp. 445-505, CRC Press, 2004.

[9] B. Smolka and A.N. Venetsanopoulos, "Noise reduction and edge detection in color images," "Color Image Processing: Methods and Applications", pp. 75-100, CRC Press, 2006.

[10] R. Lukac, "Adaptive vector median filtering," *Pattern Recognition Letters*, vol. 24, no. 12, 2003, pp. 1889-1899.

[11] B. Smolka, K.N. Plataniotis, A. Chydzinski, M. Szczepanski, A.N. Venetsanopulos and K. Wojciechowski, "Self-adaptive algorithm of impulsive noise reduction in color images," *Pattern Recognition*, vol. 35, 2002, pp. 1771-1784.

[12] B. Smolka, A. Chydzinski, K. Wojciechowski, K.N. Plataniotis and A.N Venetsanopoulos, "On the reduction of impulsive noise in multichannel image processing," *Optical Engineering*, vol. 40, no. 6, 2001, pp. 902-908.

[13] B. Smolka, "Adaptive modification of the vector median filter," *Machine Graphics & Vision*, vol. 11, no 2-3, 2002, pp. 327-350.

[14] B. Smolka, R. Lukac, A. Chydzinski, K.N. Plataniotis and K. Wojciechowski, "Fast adaptive similarity based impulsive noise reduction filter," *Real Time Imaging*, vol. 9, 2003, pp. 261-276.

[15] M.S. Moore, M. Gabbouj and S.K. Mitra, "Vector SD-ROM filter for removal of impulse noise from color images," *Proc. of the Second EURASIP Conf. (ECMCS)*, Krakow, Poland, 24-26 June, 1999.

[16] F.A. Cheikh, R. Hamila, M. Gabbouj and J. Astola, "Impulse noise removal in highly corrupted color images," *Proc. of ICIP'96 International Conference on Image Processing*, Lausanne, Switzerland, September 1996. pp. 997-1000.

[17] S.K. Mitra, T.H. Yu and R. Ali, "Efficient detail-preserving method of impulse noise removal from highly corrupted images," *Proc. of SPIE*, vol. 2182, 1994, pp. 43-48.

[18] C. Kenney, Y. Deng, B.S. Manjunath and G. Hewer, "Peer group image enhancement," *IEEE Trans. on Image Processing*, vol. 10, no. 2, 2001, pp. 326-334.

[19] B. Smolka, K.N. Plataniotis, R. Lukac and A.N. Venetsanopoulos, "Vector median based sigma filter," *Proc. of the 2003 IEEE-EURASIP Workshop on Nonlinear Signal and Image Processing (NSIP)*, Grado, Italy, June 8-11, 2003.

[20] R. Lukac, B. Smolka, K.N. Plataniotis and A.N. Venetsanopoulos, "Vector sigma filters for noise detection and removal in color images," *Journal of Visual Communication and Image Representation*, vol. 17, no. 1, 2006, pp. 1-26.

[21] J.S. Lee, "Digital image enhancement and noise filtering by use of local statistics," *IEEE Trans. on PAMI*, vol. 2, no. 2, 1980, 165-168.

[22] D.T. Kuan, A.A. Sawchuk, T.C. Strand and P. Chavel, "Adaptive noise smoothing filter for images with signal-dependent noise," *IEEE Trans on PAMI*, vol. 7, no. 2, 1985, pp. 165-177.

[23] B. Smolka, K.N. Plataniotis, "Soft-Switching Adaptive Technique of Impulsive Noise Removal in Color Images," *Lecture Notes in Computer Science*, vol. 3656, 2005, pp. 686-693

[24] B. Smolka, "On the Adaptive Impulsive Noise Attenuation in Color Images," *Lecture Notes in Computer Science*, vol. 4141, 2006, pp. 307-317

[25] M.E. Celebi, H.A. Kingravi and Y.A. Aslandogan, "Nonlinear vector filtering for impulsive noise removal from color images," *Journal of Electronic Imaging*, vol. 16, no. 3, 2007, pp. 033008.

[26] R. Lukac, "Adaptive color image filtering based on center-weighted vector directional filters," *Multidimensional Systems and Signal Processing*, vol. 15, no. 2, 2004, pp. 169-196.

[27] Y. Deng, C. Kenney, M.S. Moore and B.S. Manjunath, "Peer group filtering and perceptual color image quantization," *Proceedings of IEEE International Symposium on Circuits and Systems*, vol. 4, 1999, pp. 21-24.

[28] R. Lukac, B. Smolka, K.N. Plataniotis and A.N. Venetsanopoulos, "Vector sigma filters for noise detection and removal in color images," *Journal of Visual Communication and Image Representation*, vol. 17, no. 1, 2006, pp. 1-26.

[29] B. Smolka, "Efficient modification of the central weighted vector median filter," *Lecture Notes in Computer Science*, vol. 2449, 2002, pp. 166-173.

[30] S. Morillas, V. Gregori, G. Peris-Fajarnes and P. Latorre, "A fast impulsive noise color image filter using fuzzy metrics," *Real-Time Imaging*, vol. 11, no. 5-6, 2005, pp. 417-428.

ACKNOWLEDGMENT

This work has been supported by the Polish Ministry of Science and Higher Education under grant R13 046 02.

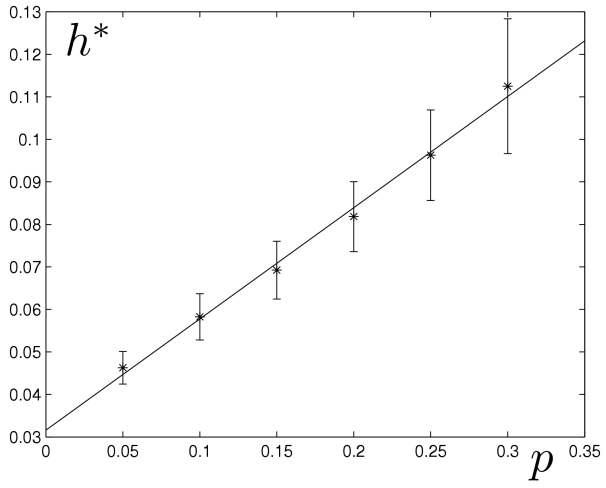

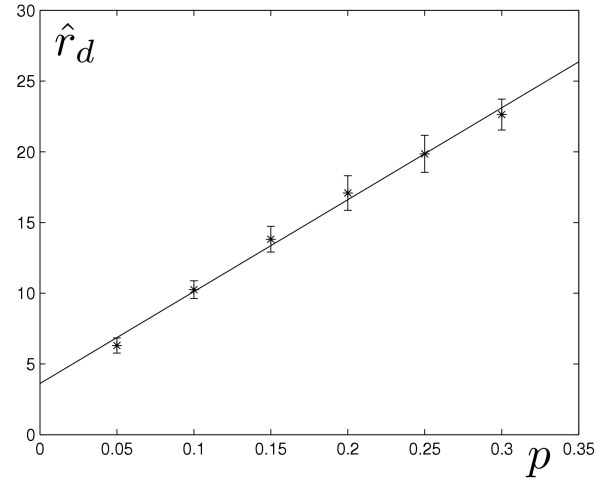

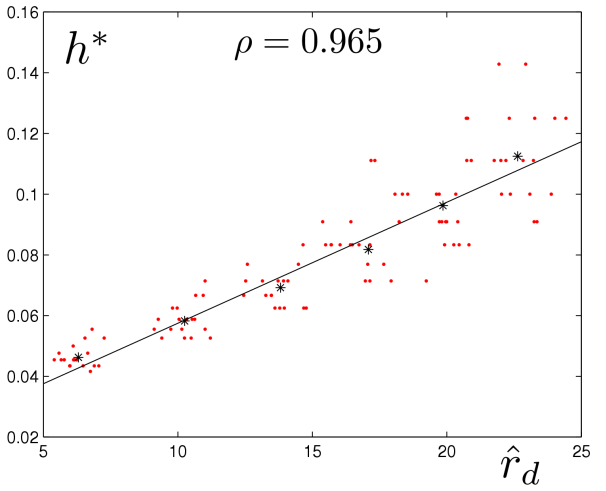

Fig. 11: Dependence between the optimal smoothing parameter h^* and the mean value $\hat{r}_d$: (a) linear dependence betweeen h^* and noise intensity p, (b) linear dependence between $\hat{r}_d$ and p, (c) linear dependence between h^* and p. In the plots (a) and (b) the standard deviations are shown and in plot (c) all data points delivered by the evaluation of 9 test images (Fig. 4) contaminated by three noise types of various intensities are depicted.

Fig. 12: Filtering efficiency: (a) parts of the test images LENA and GOLDHILL, (b) images restored with the proposed method, (c) test images distorted by respectively 15% and 10% uniform impulsive noise, (d) maps of the values of the coefficient α.

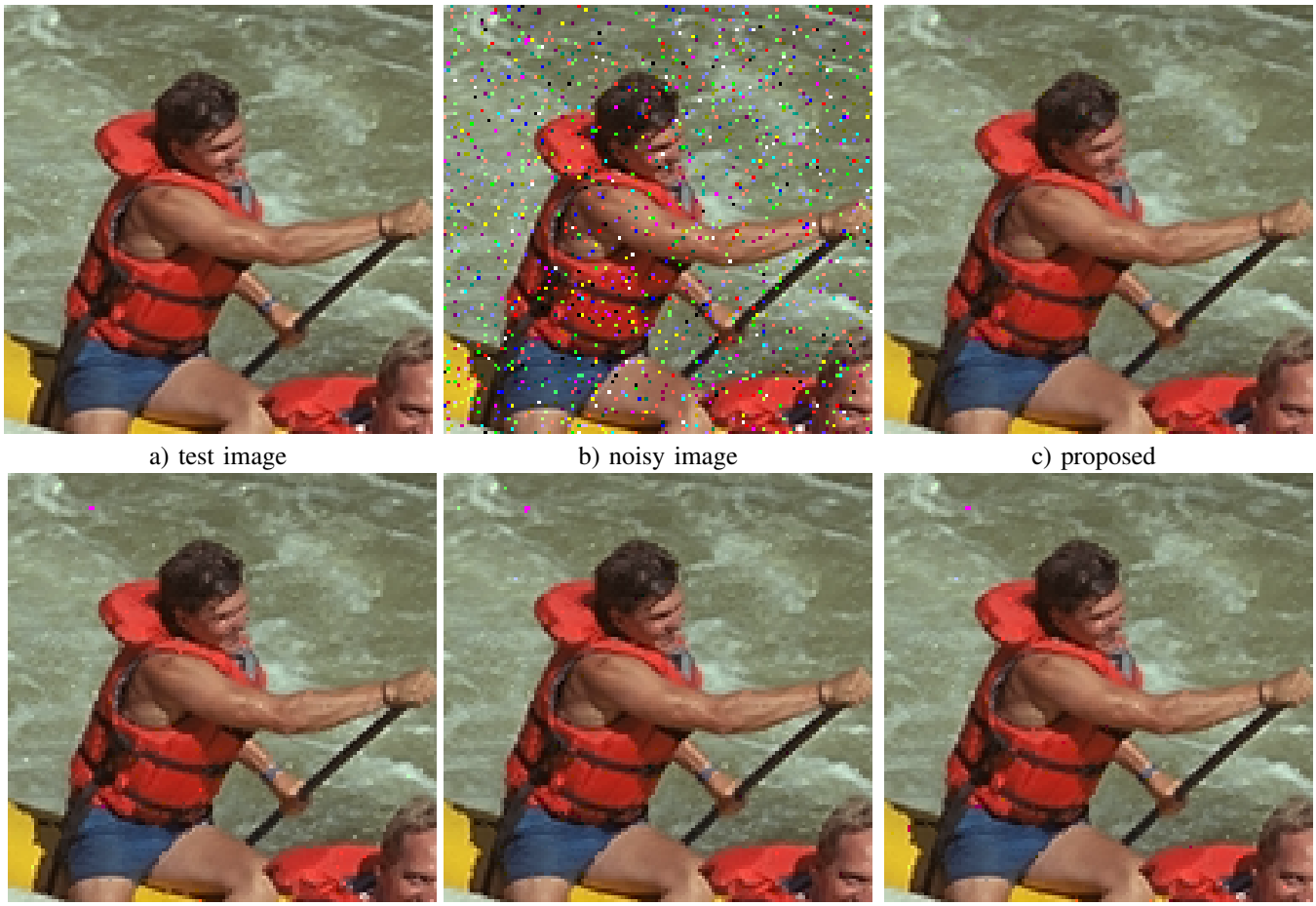

a) test image b) noisy image c) proposed

d) ACWDDF e) PGF f) SDDFr

Fig. 13: Comparison of the denoising results obtained with the new filtering technique in comparison with other filtering methods, (test image RAFTING contaminated with uniform noise, $p = 0.1$).

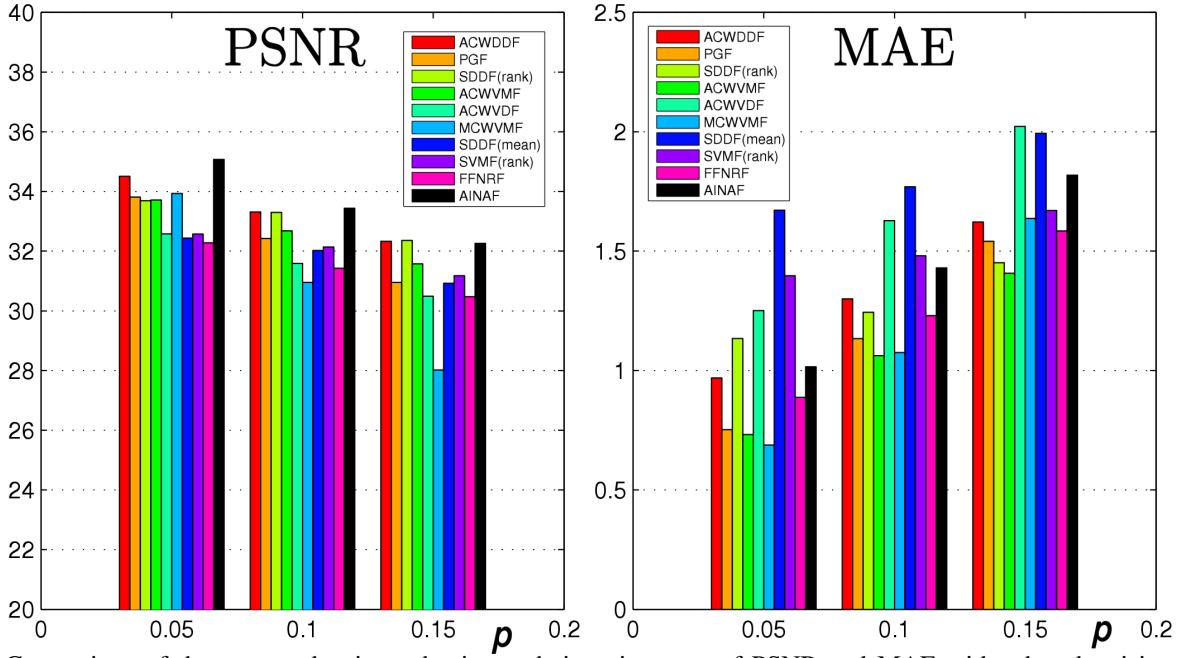

Fig. 14: Comparison of the proposed noise reduction technique in terms of PSNR and MAE with other denoising methods, (color test image RAFTING contaminated by the α noise.